

Forest Fire Risk Estimation in a Typical Temperate Forest in Northeastern China using the Canadian Forest Fire Weather Index, Case of Autumn 2019 and 2020

Maombi Mbusa Masinda

Northeast Forestry University

Fei Li

Northeast Forestry University

Qi Liu

Northeast Forestry University

Long Sun

Northeast Forestry University

Tongxin Hu (✉ htxhtxapple@sina.com)

Northeast Forestry University School of Forestry

Research Article

Keywords: fuel moisture content, weather, fire danger, Maoer mountain, forest ecosystems

Posted Date: May 7th, 2021

DOI: <https://doi.org/10.21203/rs.3.rs-481816/v1>

License:  This work is licensed under a Creative Commons Attribution 4.0 International License.

[Read Full License](#)

1 **Forest fire risk estimation in a typical temperate forest in northeastern China using the Canadian Forest Fire Weather**
2 **Index, case of autumn 2019 and 2020**

3 **Maombi Mbusa Masinda^{1,2}, Fei Li¹, Liu Qi¹, Long Sun^{1,*}, Tongxin Hu^{1,*}**

4 ¹ Key Laboratory of Sustainable Forest Ecosystem Management-Ministry of Education, College of Forestry, Northeast Forestry
5 University, 26 Hexing Road, Harbin 150040, China

6 ² Faculty of Sciences, Université Officielle de Ruwenzori, North Kivu, D.R. Congo

7 Correspondence and requests for materials should be addressed to Long Sun (sunlong365@126.com), Tel.: +86-139-4501-6458
8 or Tongxin Hu (htxhtxapple@sina.com), Tel.: +86-150-4608-9251.

9 *These authors contributed equally to this work.

10 **Abstract**

11 China's forest cover has increased by about 10% as a result of sustainable forest management since the late 1970s. The forest
12 ecosystems area affected by fire is increasing at the alarming rate of roughly 600.000 ha per year. The northeastern part of China,
13 with a forest cover of 41.6%, has the greatest percentage of acres affected by forest fires. This study combines field and satellite
14 weather data to determine factors that influence dead fuel moisture content (FMC). It assesses the use of the Canadian forest fire
15 weather index (FWI) to determine the daily forest fire danger in a typical temperate forest in northeastern China in the fall season.
16 Based on the Wilcoxon test for paired samples, the observed and predicted values of FMC showed similar variation in 63.6% of
17 sampling sites, with p-value > 0.05; and 36.4 % of sampling sites presented lower predicted values of FMC than observed values,
18 with p-value < 0.05. The Canadian Forest Fire Danger Rating System estimated the fire danger level as very low, low, moderate,
19 high, or very high in our Maoer mountain forest ecosystems.

20 **Keywords:** fuel moisture content, weather, fire danger, Maoer mountain, forest ecosystems

21 **1. Introduction**

22 Forest fires are the most widespread and critical disturbance in boreal and temperate forest ecosystems (Ying et al. 2018).
23 While China's forest cover has increased by about 10% as a result of sustainable forest management since the late 1970s (Nöchel
24 and Svennin 2017), the forest area ecosystems affected by fire is increasing at the alarming rate of roughly 600 thousand hectares
25 per year (Yang et al. 2010). Climatic conditions and forest composition in northeast China, much like those in the United States
26 of America, Canada, Australia, and Mediterranean Europe, are favourable to forest fires. The northeastern part of China
27 (Heilongjiang, Jilin, and Liaoning provinces), with a forest cover of 41.59%, has the greatest percentage of acres affected by
28 forest fires. Predictive climate models in China suggest that from 2041 to 2080, climate will be characterised by higher
29 temperature (Wu et al. 2020). Accordingly, a high priority for forest protection in China is required (Thomas 1990), and there is
30 an imperative need for China to develop its national forest fire danger rating system (Yang and Di 2011).

31 Wildfires are influenced by many factors, including vegetation, topography, weather, human behaviour, and ignition sources
32 (Flannigan et al. 2005). Great labours have been made around the world to lower the effects of wildfire including fuel diminution
33 and alteration, prescribed burning, and firebreak contour (Zong et al. 2021). However, it is particularly important to strengthen
34 forest fire management and improve forest fire prediction capabilities in regions where the forest fire danger rating system remains
35 to be developed. Ignition, spread and development of forest fires are strongly affected by the moisture content of forest fuels
36 (Rothermel 1972; Dimitrakopoulos and Papaioannou 2001). In particular, the frequency of forest fires is directly affected by the

37 moisture content of dead fuels on the ground. Therefore, accurately predicting the moisture content of dead fuels on the forest
38 surface is the key for forecasting forest fire risk and fire behaviour. Dead fine fuel moisture content varies both spatially and
39 temporally as a function of microclimate and fuel properties (Cawson et al. 2020). Temperature, relative humidity, precipitation,
40 wind velocity and solar radiation determine the moisture vapour differential between the dead fuel and atmosphere (Matthews
41 2014).

42 Aguado et al. (2007) have identified various methods estimating the FMC: the field sampling, standard fuels and
43 meteorological indices. Prediction model of fuel moisture content by the gravimetric method is often considered as the gold
44 standard approach (Matthews 2010). Nevertheless, this approach has limited use as it cannot provide continuous or real-time
45 moisture data when desired and needs continuous equipment and workers in the field (Cawson et al. 2020). The method that used
46 standard fuels is based on monitoring weight changes of previously calibrated surface forest fuels that are presumed to be good
47 representatives of certain fuel sizes. It reduces the effort of field sampling and provides an instant estimation of FMC. However,
48 this method has a little spatial significance as the measurements are limited (Aguado et al. 2007). Meteorological danger indices
49 method is often used to measure dead FMC. These indices depend on present and past meteorological conditions, since they try
50 to evaluate the drought of different forest fuels. It leads to frequent updating and, in addition to estimating FMC, offers other
51 critical variables for fire management. Based on the last method, this study used the FMC meter to evaluate the change of the
52 FMC as it instantly evaluate the change of FMC in any place; however it also needs manual measurement before or after the
53 experiment (Masinda et al. 2021).

54 Prediction of forest fire has been studied for decades using different forest rating systems like the Canadian Forest Fire Danger
55 Rating System (CFFDRS), U.S. Forest Service National Fire Danger Rating System (NFDRS), and McArthur Forest Fire Danger
56 Index -FFDI- (Di Giuseppe et al. 2016). Although a wide range of indices has been developed to calculate fire risk (Bett et al.
57 2020), many are limited to specific areas while some indices are valid on a large scale like the fire weather index (FWI). The
58 CFFDRS has, since the early 20th century, involved an extensive network of weather observations, FMC field sampling, and
59 ignition sustainability investigations (Fujioka et al. 2008). The FWI system is a sub-system of the CFFDRS (de Groot and Groot
60 1987). The FWI was established by Van Wagner (1974) and is more efficient than other forest fire indices (Schunk et al. 2017;
61 Tremblay et al. 2018). It predicts the FMC by relying on meteorological variables from different global regions. It then combines
62 these variables to analyse fire behaviour in terms of spread and intensity (Vitolo et al. 2019). It also determines the effects of
63 meteorological variables on forest fuels and forest fires by providing a relative numerical rating of fire danger over a given area.
64 However, it is not able to describe a complete picture of daily wildfire danger with a single number (Stocks et al. 1989).

65 Initially developed for use in Canadian pine stands, FWI sees widespread use in other forest stands due to its simplicity of fit.
66 The FWI system is widely approved by many fire and land management agencies, which use it to issue fire warnings and assign
67 resources in the field (Dimitrakopoulos et al. 2011; Vitolo et al. 2019), but it only offers a qualitative overview of predicted fire
68 regimes. Many studies have established a strong relationship between FWI codes/indices and fire occurrence and behaviour
69 (Papagiannaki et al. 2020). Simpson et al. (2014) argued the necessity of evaluating the suitability of applying the FWI system to
70 regions other than the one in which it was originally established. Accordingly, this work attempted to provide insights on the
71 following questions: Which weather variables influenced much the fuel moisture content in Maoer mountain forest ecosystem?
72 Does the relationship between the moisture of the FMC meter and China Weather Satellite Station (CWSS) change by forest type
73 and time? What is the rating of fire danger in the fall fire-prone season? Thus, it aimed to determine the main meteorological
74 factors influencing FMC in a typical temperate forest in northeastern China and to assess the potential use of the Canadian Forest
75 Fire Weather Index as a decision-support tool in fire hazard management.

76 2. Material and method

77 2.1. Study location

78 This study was conducted in a typical temperate forest of Maoer mountain, in northeastern China (45°43'N, 126°37'E; average
79 elevation is 255 m). The surface area of Maoer mountain forest ecosystem is 21813.1 ha. The region features a cold, temperate
80 climate, with rainy summers. It receives an average annual rainfall of 649 mm. The hottest month in this area is July, with an
81 average temperature of 21.8°C, while January is the coldest month with an average temperature of -19.9°C. The annual thermal
82 amplitude is 41.7°C and the rainfall amplitude is 171 mm. The bedrock is granite and the soil is mainly dark brown forest soil
83 (Wang 2006). Since the beginning of the 20th century, the primary forest has been gradually degraded by large-scale industrial
84 logging by Russian and Japanese invaders as well as by the Chinese government. The primary forest, which was dominated by
85 *Pinus koraiensis* Siebold and Zucc. mixed with deciduous species such as *Betula platyphylla* Sukaczew, *Larix gmelinii* L., *Populus*
86 *davidiana* Dode, *Quercus mongolica* Fisch., and *Fraxinus mandshurica* Rupr., has been replaced by a secondary forest and mostly
87 by *L. gmelinii* plantations (Chen et al. 1982). Currently, there are three main types of secondary forest distributed in various sites
88 characterised by different conditions. These forests are forest of *Quercus mongolica* on steep upper slope arid and infertile, the
89 mixed deciduous forest located at well-drained fertile gentle mid-slope and the deciduous forest on gentle slope moist, and fertile.
90 There are also two dominant plantations: *L. gmelinii* and *P. koraiensis* plantations (Wang 2006). In the winter, the temperature is
91 low, the snow is frozen, and there are no burning conditions, so forest fires are registered during these periods. The mean annual
92 area of burnt forest in Heilongjiang Province varies between 500 and 2500 km² (Li et al. 2015). These averages represent 0.25 -
93 1.2 % of the total forest cover (205,328 km²) of Heilongjiang Province estimated as in the China forest administration website
94 (12 December 2019).

95 2.2. Meteorological data acquisition and use

96 This study used data from FMC meters which provide measurements of meteorological variables and the fresh weight of fuel
97 on the ground surface (Masinda et al. 2021). It also used data from the CWSS as the installation of FMC meters over large areas
98 of forest requires a lot of resources (material, financial, temporal and human). The first series of data was acquired from the FMC
99 meters in the field. FMC meters were set in Maoer mountain forest ecosystem to track the change of dead fuel moisture content
100 in relation to variations in air temperature, relative humidity, solar radiation, wind speed, and rainfall. We acquired the second
101 series of data from the CWSS -Harbin Station- (<http://cdc.cma.gov.cn/>, station id: 50953, 45.45°N and 126.46°E), which included
102 temperature, relative humidity, wind speed and total daily rainfall. The temporal and spatial resolution of CWSS are respectively
103 one hour and seventy-one kilometres. These series of data served to develop the FMC patterns and to calculate the FWI indices
104 (noon temperature, relative humidity, wind speed, and total daily rainfall).

105 2.3. Sampling

106 It is rarely practical to measure the dead fuel moisture content directly in the field; thus, it is generally estimated. It is possible
107 to use either real or predicted values of air relative humidity and temperature to reasonably estimate the FMC (De Melo-Abreu
108 et al. 2010). In this study, we used the FMC meter which is a device consisting of an automatic balance and a mini weather station.
109 It automatically measures the fresh fuel mass, air temperature, relative humidity, wind speed, solar radiation, and rainfall reaching
110 the fuels on the ground surface (as well as soil moisture and temperature) at an instantaneous time interval. It supplies a continuous
111 and automated measurement of the FMC that can be transferred from remote sampling site, reducing the manpower required to
112 get information on the variation of the moisture content in the field.

113 Data were collected at 11 sampling points (5 and 6 sampling plots in 2019 and 2020, respectively) arranged on four linear
 114 transects (Table 1). Transects were separated by 1.11 km, or 0.01 degree of latitude and sampling points on each transect were
 115 distant one of the other of 0.788 km, corresponding to 0.01 degree of longitude at 45 degree of latitude. Around each sampling
 116 point, we had plotted a quadrant of 50 meters side which was used to describe the vegetation around it. In each quadrant, we
 117 manually gathered samples of dead fine surface fuels over an area of 30 cm × 30 cm along the transect, equivalent of the FMC
 118 basket meter. Samples were composed of twigs of one hour time-lag and freshly fallen nonwoody material which includes leaves,
 119 cones, pollen cones (Keane 2015). We then oven-dried our samples at 105°C for 24 hours and determined the moisture content
 120 as the fraction of water mass (W_f) to oven-dry fuel mass (W_d):

$$121 \quad FMC_{(1)} = [(W_f - W_d) / W_d] \times 100 \quad (1)$$

122 To estimate the moisture content of fine dead fuel using the FWI system (Wotton 2009), we deduced the predicted values of
 123 the FMC using the Fine Fuel Moisture Code (FFMC) according to the following formula:

$$124 \quad FMC_{(2)} = 147.2 \times (101 - FFMC) / (59.5 + FFMC) \quad (2)$$

125 **Table 1** Local field sampling characteristics

126 In this table, D denotes the depression while TH represents the tree height.

Site	Longitude	Latitude	Tree species composition	Aspect	Slope	D	TH
1	127.65	45.40	<i>Betula platyphylla</i> Sukaczew, <i>Populus davidiana</i> Dode and <i>Fraxinus mandshurica</i> Rupr.	North	15	0.7	18
2	127.69	45.41	<i>Betula platyphylla</i> , <i>Populus davidiana</i> , <i>Tilia mandshurica</i> Rupr. and Maxim. and <i>Juglans mandshurica</i> Maxim.	West	10	0.8	17
3	127.66	45.41	<i>Fraxinus mandshurica</i> , <i>Juglans mandshurica</i> , <i>Phellodendron amurense</i> Rupr., and <i>Ulmus pumila</i> L.	Northwest	15	0.7	16
4	127.67	45.41	<i>Fraxinus mandshurica</i> , <i>Juglans mandshurica</i> , <i>Tilia mandshurica</i> , <i>Populus davidiana</i> , <i>Betula costata</i> Trautv, <i>Ulmus pumila</i> , etc.	Northwest	15	0.6	17
5	127.68	45.41	<i>Populus davidiana</i> , <i>Tilia mandshurica</i> , <i>Juglans mandshurica</i> , <i>Betula costata</i> and <i>Fraxinus mandshurica</i>	Southeast	15	0.8	18
6	127.67	45.43	<i>Fraxinus mandshurica</i> , <i>Juglans mandshurica</i> , <i>Phellodendron amurense</i> Rupr., <i>Betula platyphylla</i>	North	14	0.7	17
7	127.66	45.42	<i>Larix gmelinii</i> and <i>Ulmus propinqua</i>	Southeast	10	0.7	18
8	127.66	45.40	<i>Quercus mongolica</i> Fisch. and Ledeb.	South	11	0.8	14
9	127.70	45.41	<i>Pinus sylvestris</i> , <i>Betula platyphylla</i> and <i>Ulmus propinqua</i>	Southeast	9	0.6	15
10	127.67	45.41	<i>Ulmus propinqua</i> , <i>Juglans mandshurica</i> , <i>Quercus mongolica</i>	Northeast	12	0.7	16
11	127.67	45.42	<i>Ulmus propinqua</i> , <i>Fraxinus mandshurica</i> , <i>Phellodendron amurense</i>	Northwest	13	0.8	17

127 **2.4. Modelling with data from FMC meters**

128 To assess the FMC variation, we fitted general linear models to select variables that have a strong effect on FMC. The FMC
 129 meter dataset consisted of air temperature, relative humidity, wind velocity, solar radiation and fresh fuel weight. The CWSS
 130 dataset included the temperature on the ground surface, temperature at 10 meters height, sunshine-hours, relative humidity,
 131 rainfall and wind velocity. Before computed FMC models, variable importance was first determined using the random forest
 132 method and was presented by a graph. Collinearity was checked for each model; thus, FMC models were developed. All models
 133 were computed in RStudio version 1.1.453.0 (RStudio Inc. 2018) and fuel moisture content variation was drawn with
 134 OriginPro2018 (Origin Lab, Northampton, MA, USA).

135 2.5. FWI codes/indices prediction and correlation

136 Estimation of FWI indices and codes was obtained using *fwi-function* with the *cffdrs-R* package (RStudio Team 2018;
 137 Integrated Development for RStudio, Inc., Boston, MA) based on noon local standard time weather observations, including
 138 temperature, relative humidity, wind speed, 24-hour rainfall, and the previous day’s fuel moisture conditions (Wang et al. 2019).
 139 These codes and indices are respectively the fine fuel moisture code (FFMC), duff moisture code (DMC), drought code (DC),
 140 build-up index (BUI), and initial spread index (ISI). The daily severity rating (DSR) is an additional component of the FWI
 141 system, planned to be more directly related to the probable effort required for wildfire suppression, and it is a power conversion
 142 of FWI that underlines high FWI values (Tsinko et al. 2018). We used the qualitative Forest Fire Danger Rating System as
 143 established by Van Wagner (1987) to describe the fire danger as very low, low, moderate, high, very high, or extreme (Table 2).

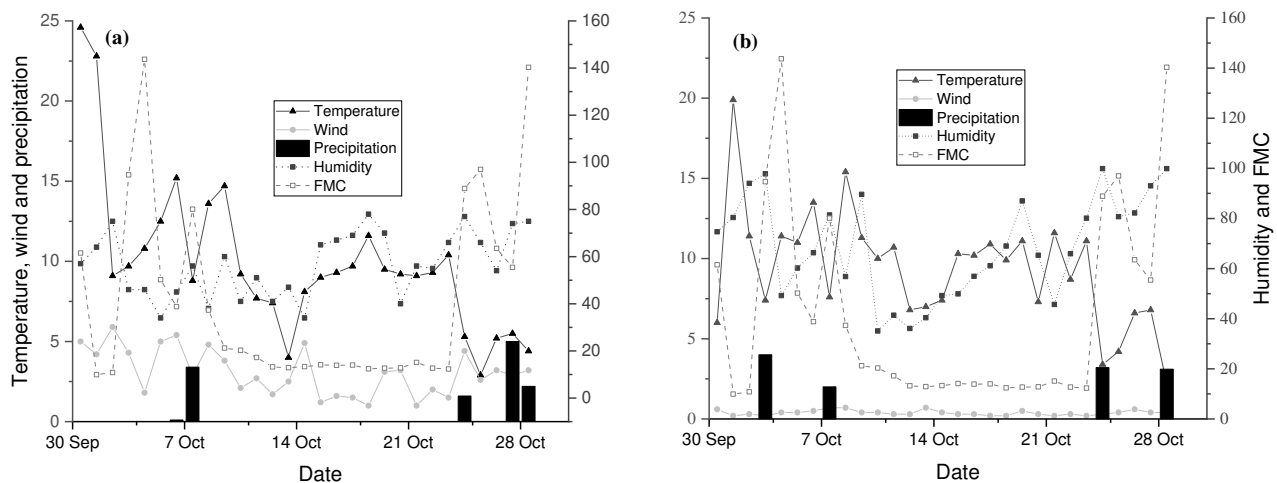
144 **Table 2** Fire danger rating scale

Danger classes	FWI range
Very low	00 - 01
Low	02 - 04
Moderate	05 - 08
High	09 - 16
Very high	17 - 29
Extreme	30 +

145 **3. Results**

146 3.1. Response of FMC variation to weather factors

147 Our results showed that, relatively, the FMC was more sensitive to rain, less sensitive to relative humidity and temperature,
 148 and insensitive to wind speed (Fig. 1- a, b). In addition, the FMC response to a rainfall of 2 - 4 mm during a good drying day took
 149 2-3 days for the FMC to recover the pre-rain values. These results highlight the strength of the relationship between rain and
 150 FMC variation.

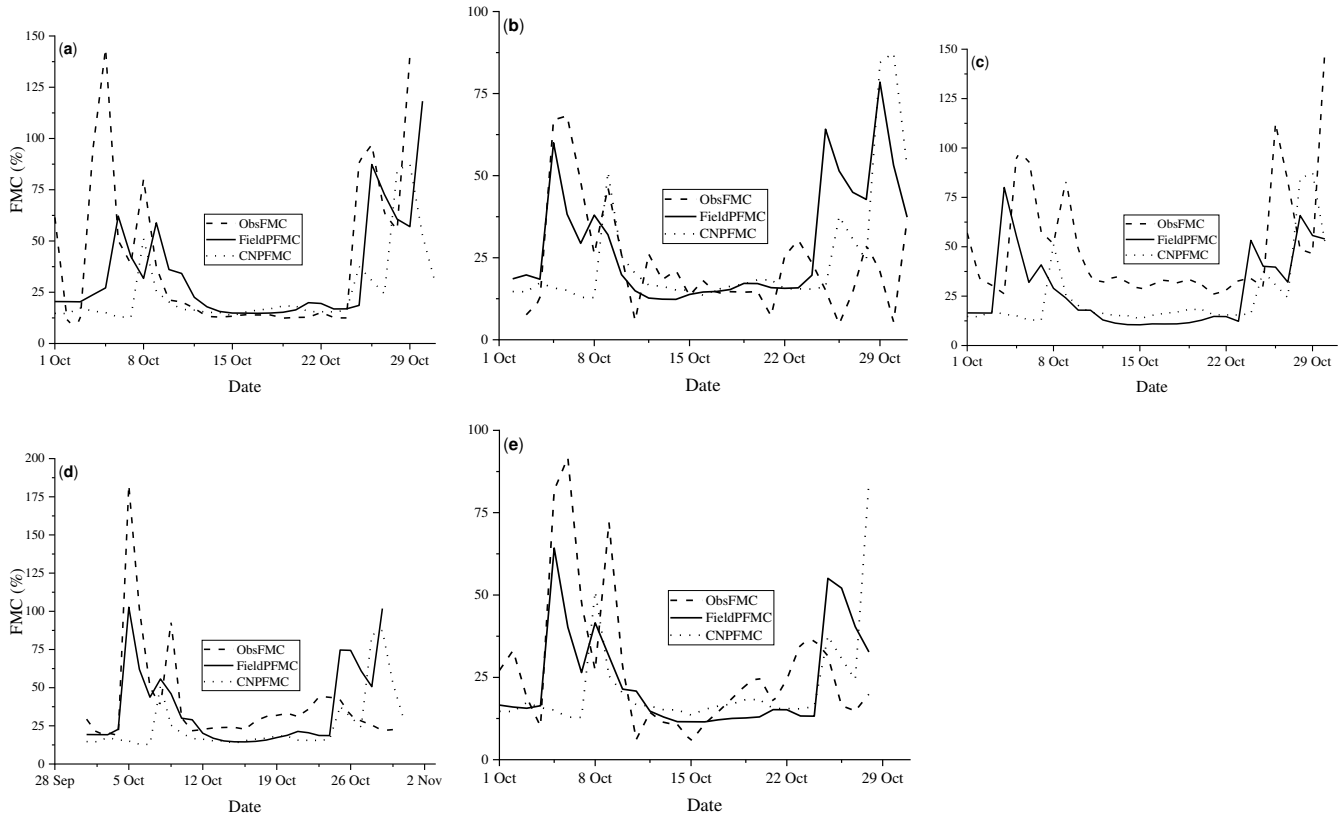


151
 152 **Fig. 1** Variation of FMC based on (a) FMC meter and (b) China Weather Station database

153 3.2. Comparison among noon FMC

154 In this paragraph, we compare the changes of FMC with field measurements, predicted field FMC and predicted CWSS FMC.
 155 Results are shown in Fig. 2-a, b, c, d, e. In 2019, the period from 11 to 25 October presented low FMC values (Fig. 2). On the
 156 other hand, the first and the last week of the month presented high values of FMC, mainly due to rain. In 2020, results in Fig. 3-
 157 a, b, c, d, e, f showed that the predicted (FMC meter and CWSS) FMC varied at the same rate as the measured FMC although, a
 158 dizzying increase in FMC was observed after the rain of October 20. The maximum value of FMC approached 325% (Fig. 3-e)
 159 while the minimum FMC value was 7.4% (Fig. 3-b).

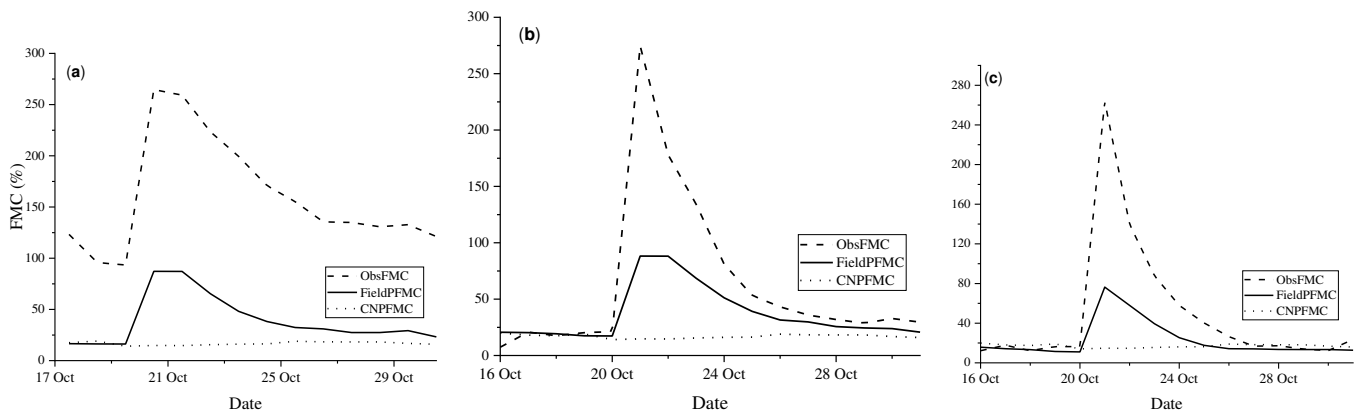
160

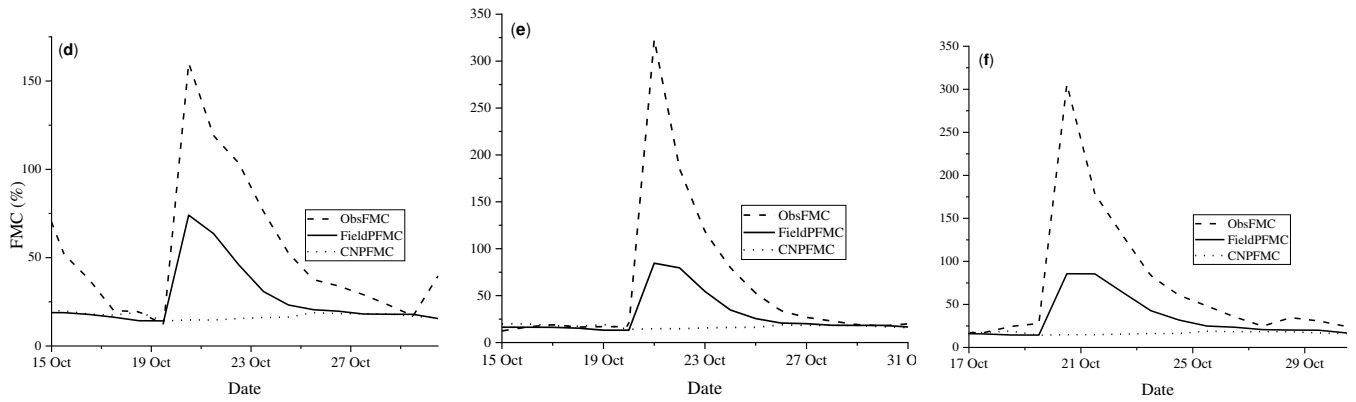


161

162 **Fig. 2-a, b, c, d, e** Observed versus FMC meter and CWS predicted FMC, in 2019

163





164
165 **Fig. 3-a, b, c, d, e, f** Observed versus FMC meter and CWSS predicted FMC, in 2020

166 3.3. Patterns of fuel moisture content

167 3.3.1. Predicted model with both data sources

168 The general linear model developed with both FMC meter and CWSS variables showed that rain and relative humidity
169 influence on FMC were strong than the influence of temperature, wind speed, solar radiation and sunshine time. All models
170 presented a good predictive power ($R\text{-sq. adj.} > 70$). In the fitted models (Table 3), T , H , W , Rn , and R respectively denote the
171 temperature, relative humidity, wind speed, rain and solar radiation from the FMC meter and SS the sunshine timing and T_h
172 the temperature at 2 m height for the CWSS data source. The residual standard error (RSE) varied from 15.72 to 31.17; the F-statistic
173 varied between 34.28 and 74.15 while the degree of freedom (DF) oscillated between 26 and 29.

174 **Table 3** FMC models fitted with FMC meter and CWSS data

Model	Equation	RSE	R-sq. (adj.)	F	DF
1	$FMC = 25.29 Rn + 3.77 SS$	31.17	0.70	34.28	27
2	$FMC = 2.989 SS$	15.72	0.71	74.15	29
3	$FMC = 1.165 H - 4.536 T + 0.180 R$	20.19	0.88	73.56	27
4	$FMC = 0.491 H + 0.130 Rn^5$	26.73	0.72	40.39	28
5	$FMC = 2.647 T_h + 0.235 Rn^4$	17.26	0.76	44.20	26

175 3.3.2. Predicted model with FMC meter data

176 Apart from developed models in the above section, we computed daily and diurnal models of FMC in order to observe if the
177 effect of sun would increase the quality of the model. Thus, in each site FMC models were developed in 2019 and 2020 with
178 diurnal or daily data.

179 Developed models in 2019 showed that relative humidity, temperature, wind speed and solar radiation influenced the water
180 content of fuels in site 1. In site 2, humidity, temperature and wind speed are the influential factors. In sites 3, 4 and 5, wind speed
181 and rain did not result in a substantial improvement in model efficiency. A general overview on daily developed FMC models
182 proved that relative humidity, temperature, solar radiation and wind velocity influenced much the FMC. The integration of rain
183 ($p\text{-value} > 0.05$) did not result in a substantial improvement in model efficiency. Out of five sampling sites, one was characterised
184 by a high predictive power model: $R\text{-sq. (adj.)} = 0.70$. The other four sites were characterised by models with medium predictive
185 power: $0.52 \leq R\text{-sq. (adj.)} \leq 0.64$ (Table 4).

186 Developed models with diurnal data showed that relative humidity, temperature and solar radiation had a strong effect on
 187 FMC. The influence of wind velocity and rain were not noticeable. Results in Table 5 showed that sites 1, 2 and 3 were
 188 characterised by models with high predictive power: $0.72 \leq R\text{-sq.}(adj.) \leq 0.80$ while sites 4 and 5 were characterised by models
 189 with medium predictive power: $0.50 \leq R\text{-sq.}(adj.) \leq 0.55$. The residual standard error is RSE oscillated between 0.35 and 34.97
 190 for daily developed models and 0.29 to 31.71 for diurnal developed models in Table 4. The F-statistic varied between 337.6 to
 191 787.6 ($773 \leq DF \leq 1016$) for daily fitted models and F-statistic shifted between 138.3 and 664.1 ($408 \leq DF \leq 540$), etc.

192 Daily developed models of FMC in 2020 indicated that relative humidity, rain and temperature were the most important
 193 factors influencing the water content of fuels in all sampling sites. The effect of wind on water content was significant in site 1
 194 and the effect of solar radiation was only influential in site 3. Two of six sampling sites were characterised by models with high
 195 predictive power: $0.73 \leq R\text{-sq.}(adj.) \leq 0.83$. The other four sites were characterised by models in medium predictive power: 0.52
 196 $\leq R\text{-sq.}(adj.) \leq 0.66$ (Table 6). In addition, developed models with diurnal data showed that relative humidity, temperature and
 197 rain were the influencing drivers of FMC. Three sites were characterised with models in high predictive power, $R\text{-sq.}(adj.) > 0.70$
 198 and three others with medium predictive power: $0.61 \leq R\text{-sq.}(adj.) \leq 0.66$ (Table 7).

199 **Table 4** Daily developed FMC models in 2019

Model	Equation	RSE	R-sq.(adj.)	F	DF
1	$FMC = 0.648 H - 2.491 T + 30.119 W + 0.043 R$	34.97	0.64	343.3	773
2	$FMC = 0.130 H + 1.241 T + 1.543 W$	17.12	0.57	427.5	984
3	$FMC = 0.008 H - 0.007 T + 0.0004 R$	0.35	0.70	678.3	880
4	$FMC = 0.347 H + 0.003 R$	25.27	0.61	787.6	1016
5	$FMC = 0.237 H + 1.243 T + 0.001 R$	24.21	0.52	337.6	943

200 **Table 5** Diurnal developed FMC models in 2019

Model	Equation	RSE	R-sq.(adj.)	F	DF
1	$FMC = 0.979 H - 1.735 T$	31.71	0.72	599.9	469
2	$FMC = 0.134 H - 0.156 T^2 + 4.915 T - 0.029 T \cdot H$	15.38	0.72	277.4	423
3	$FMC = 0.013 H - 0.010 T + 0.00023 R$	0.29	0.80	664.1	496
4	$FMC = 0.456 H + 0.019 R$	31.68	0.55	334.9	540
5	$FMC = 0.481 H + 2.620 T - 0.046 T \cdot H$	29.85	0.50	138.3	408

201 **Table 6** Daily developed FMC models in 2020

Model	Equation	RSE	R sq.(adj.)	F	DF
1	$FMC = 1.982 H - 2.499 T + 59.368 W + 85.949 Rn$	87.97	0.83	848.4	692
2	$FMC = 0.808 H - 1.132 T^2 + 54.249 Rn^2$	55.06	0.63	420.0	741
3	$FMC = 0.882 H - 2.968 T + 46.989 Rn + 0.044 T \cdot H$	42.56	0.65	402.1	857
4	$FMC = 0.722 H + 22.438 Rn$	35.18	0.73	1220.0	886
5	$FMC = 0.952 H^2 + 64.02 Rn$	81.29	0.52	550.2	1007
6	$FMC = 0.830 H + 54.805 Rn$	55.52	0.66	715.8	740

202 **Table 7** Diurnal developed FMC models in 2020

Model	Equation	RSE	R sq.(adj.)	F	DF
1	$FMC = 2.288 H - 2.866 T$	82.41	0.82	529.3	230
2	$FMC = 1.164 H - 3.647 T + 48.114 Rn$	53.25	0.64	151.3	251
3	$FMC = 1.165 H - 7.686 T + 0.159 T \cdot H$	38.07	0.74	245.9	260
4	$FMC = 0.959 H - 1.102 T^2$	33.74	0.76	475.4	301
5	$FMC = 1.257 H - 3.757 T + 62.70 Rn$	58.67	0.61	143.4	272
6	$FMC = 1.219 H - 2.260 T + 46.572 Rn$	55.05	0.66	162.3	245

203 3.4. Adequacy of the FWI system in predicting the FMC in Maoer mountain forest ecosystem

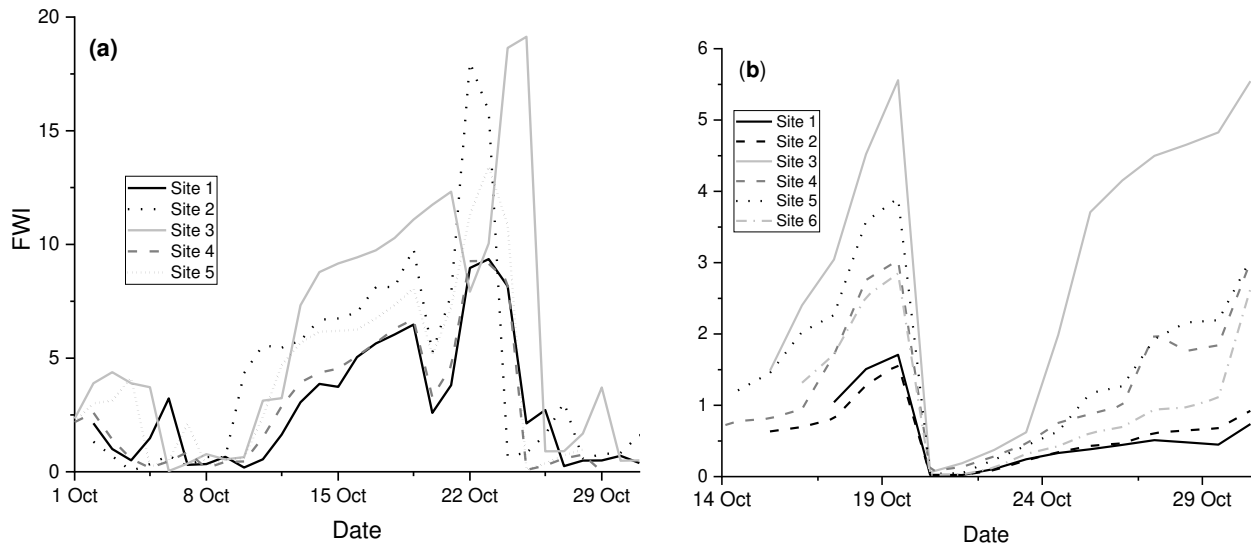
204 The Wilcoxon test for paired samples showed that the observed and predicted values of FMC in 2019 were similar in sites 1,
 205 2, and 5 ($p\text{-value} > 0.05$) and different in sites 3 and 4 ($p\text{-value} < 0.05$). Note that the predicted FMC values were calculated with
 206 the FWI function. In 2020, the Wilcoxon test for paired samples showed that the moisture content predicted with FMC meter data
 207 were significantly different to the moisture content predicted with CWS data in sites 1, 2 and 6 ($p\text{-value} < 0.05$). In sites 3, 4 and
 208 5, both moisture contents were similar ($p\text{-value} > 0.05$). The difference between the observed and estimated FMC in site 1, 4 and
 209 6 would be influenced by canopy density, altitude, slope, aspect or may be related to sampling facts rather than to real variance
 210 in moisture content (Table 8).

211 **Table 8** Wilcoxon's test result for paired samples between the observed and predicted FMC

Sites	Estimated parameter (V)	p-value	Sites	Estimated parameter (V)	p-value
1	248	> 0.05	1	101	< 0.001
2	206	> 0.05	2	134	< 0.001
3	465	< 0.001	3	59	> 0.05
4	129	> 0.05	4	109	> 0.05
5	122	> 0.05	5	100.5	> 0.05
-	-	-	6	105	< 0.05

212 3.5. Fire danger estimation

213 The value of FWI varied across the study period (October 2019) was low from October 1st-12th, moderate from October 13th-
 214 18th, very high from October 19th-26th, and low from October 26th-31st. It had rained only during the first and last week of the
 215 study period. The lack of rain was mainly responsible for the high fire danger ratings. Fig. 4-a depicts that the FWI values in sites
 216 2 and 3 from October 21st-25th reached a high or a very high level of fire danger, while FWI values in sites 1, 4, and 5 varied
 217 between the very low and the moderate fire danger level. Results in Fig. 4-b illustrate that from 14 to 31 October 2020, the FWI
 218 oscillated between 0 and 5.56. Unfortunately, the value of FWI from 14 to 31 October in 2020 was lower than in 2019 in the
 219 same time interval.



220

221 **Fig. 4** Variation of FWI in 2019 (a) and 2020 (b)

222 **4. Discussion**

223 In this paper, we analysed the FMC variation and fire danger in typical temperate forests in order to (i) identify the most
 224 important variables affecting FMC changes and (ii) evaluate the skill of the FWI system in predicting forest fire risk in temperate
 225 forest stands, in northeastern China.

226 *4.1. FMC changes*

227 There were weighty increases in FMC during rainfall (Fig. 1- a, b). Although there were some divergences in FMC
 228 presentation, all data sources displayed similar FMC changes and provided the same information to researchers and fire managers.
 229 The difference between field (45.41°N, 127.67°E) measures and those obtained from CWSS (45.45°N, 126.46°E) is presumably
 230 related to the distance between the station and the experimental area. Thus, an increase in number of weather stations in fire-
 231 prone regions is needed as suggested by Chuvieco et al. (1999, 2002) and Zhang et al. (2011).

232 The FWI system underestimated the FMC values, compared to field-experimental observations (Fig. 2 and 3). The disparity
 233 between observed and predicted values may be a result of the height at which wind speed was sampled, which differed between
 234 the field measurements and the estimated values. Tree canopy may also play a role in this difference. We measured temperature
 235 and wind speed at 0.3 m above the ground under tree cover, while the FWI system measures temperature at 2 m and wind speed
 236 at 10 m in an open area (Field 2020). Accordingly, previous studies have shown that tree canopy reduces solar radiation and wind
 237 flow on the ground surface and has an effect on dead fuel moisture content (Zylstra 2011; Estes et al. 2012; Zhang et al. 2017).

238 *4.2. FMC meter data prediction*

239 Different sites revealed variability in the accuracy of FMC predictors. Relative humidity, temperature and/or solar radiation
 240 had a significant effect on FMC in these sites. Diurnal models were more accurate than daily models, however FMC drivers were
 241 the same in both models. After a 2 - 4 mm rainfall, the FMC needed 2 - 3 days to recover its pre-rainfall values. Thus, we
 242 hypothesised that firefighters could spend two to three days without raids in the field as dead fuels would be too wet to burn for
 243 approximately two to three days after the rainfall event. During this period, the fuel water content exceeded the ignition and fire

244 spread threshold of all types of fuel in the region (Masinda et al. 2020). Comparison between observed and predicted FMC
245 showed that the observed values were slightly greater than the predicted values but were not significantly different (Table 8).
246 Results of 2019 and 2020 allowed us to adopt the use of both data sources to predict the moisture content of dead fine surface
247 fuels in Maoer mountain forest ecosystem because at eleven sampling sites, the predictions were statistically similar in seven
248 sites, i.e. 63.6%.

249 *4.3. Validity of the FWI system for fire risk management in typical temperate forests in China*

250 Our FWI values were similar to those of other Chinese provinces where the FWI values were linked to fire (Lynham and
251 Stocks 1989; Tian et al. 2011, 2014; Yang and Di 2011). More studies had found a strong relationship between FWI and wildfire
252 occurrence in other regions, like the Mediterranean, south-east and Central Europe (Good et al. 2008; Dimitrakopoulos et al.
253 2011; De Jong et al. 2016; Bedia et al. 2018; Lahaye et al. 2018; Fernandes 2019), Russia (Tosic et al. 2019), Australia (Dowdy
254 et al. 2010), and on the global scale (Field et al. 2015). Our results showed that the FWI value in the interval from October 21 to
255 28 exceeded 13.95 and approached 20.67, which corresponds to more than 30 and 170 ha of burnt forest, respectively, according
256 to Xanthopoulos et al. (2014) scale. The FWI system has produced valuable insight for fire management by determined very low,
257 low, medium, high and very high level of fire danger in Maoer mountain forest ecosystem. It improves the accuracy of fire hazard
258 assessment in the study area by informing the public of imminent fire hazards; thus, it is a useful tool to regulate access to forest
259 ecosystems during the fire-prone season.

260 The spatial distribution of FWI indices differs considerably across the globe. Although FWI values can be calculated at any
261 location based on weather variables, however, they are only useful where fuels are available (Vitolo et al. 2019). Considering the
262 heterogeneity of forest ecosystems and the uncertainty of future trends in fire severity and intensity, which is largely due to
263 complex, non-linear interactions among weather, forest, and anthropogenic factors, specific information about vegetation type
264 vulnerability is needed on both local and global scales (Flannigan et al. 2009; Papakosta and Straub 2017; Fernandes 2019).

265 *4.4. Implication for wildfire management*

266 The FMC meters serve to track the moisture content of dead fuel over time in a range of landscape locations without the need
267 of frequent study area visits. They are more precise than distant weather stations, particularly in different locations with different
268 forest ecosystems. However, they should be used in concert with other tools as sometimes they can't track data when their batteries
269 are discharged. Many humidity models used by fire managers had been established with data from weather stations remote from
270 sampling sites, so FMC meters are valuable in this regard. The challenge we have is to equip the FMC meter with all its
271 components necessary to collect all the useful data, even remotely.

272 **5. Conclusion**

273 This study evaluates the aptitude of the Canadian Forest Fire Weather Index in estimating fire danger in typical temperate
274 forest stands in the northeast of China. Before evaluation, we developed FMC models with FMC meter and CWSS data. From
275 this dataset, we determined the most important weather variables responsible for changes in fuel moisture content. FMC meter
276 data were more accurate in estimating fire danger than CWSS data, suggesting more local meteorological stations in fire-prone
277 regions would be beneficial in fire-risk assessment. In four of five models, rain had the strong effect on the variation of FMC.
278 Relative humidity, temperature, and solar radiation also had a relative effect on FMC. Among models built from field data, there
279 was variation in factors affecting FMC. Relative humidity was the most important factor, followed by radiation, temperature, and

280 rainfall. The Canadian Forest Fire Danger Rating System estimated the fire danger level as very low, low, moderate, high, or very
281 high in our Maoer mountain forest ecosystems.

282 **Acknowledgments:**

283 We sincerely thank Professor Wang Chuankuan, Director of the Global Ecology Laboratory at Northeast Forestry University
284 for providing us rainfall data. We also thank Ms. Zhang Yujing for her collaboration. We would like to thank Elizabeth Tokarz
285 of Yale University and Chula Mwagona Patteson for their assistance with spell checking and grammar editing.

286 **Funding**

287 This work was carried out within the framework of the National Key Research and Development Program of China, Key
288 Projects for Strategic International Innovative Cooperation in Science and Technology (2018YFE0207800) and was partly
289 sponsored by the China Scholarship Council (CSC No.2016DFH417).

290 **Competing interests:** The authors declare there are no competing interests.

291 **References**

- 292 Bedia J, Golding N, Casanueva A, et al (2018) Seasonal predictions of Fire Weather Index: Paving the way for their operational
293 applicability in Mediterranean Europe. 9:101–110. <https://doi.org/10.1016/j.cliser.2017.04.001>
- 294 Bett PE, Williams KE, Burton C, et al (2020) Skillful seasonal prediction of key carbon cycle components: NPP and fire risk.
295 Environ Res Commun. <https://doi.org/10.1088/2515-7620/ab8b29>
- 296 Cawson JG, Nyman P, Schunk C, et al (2020) Estimation of surface dead fine fuel moisture using automated fuel moisture sticks
297 across a range of forests worldwide. Int J Wildl Fire. <https://doi.org/10.1071/WF19061>
- 298 Chen DK, Zhou XF, Zhao HX, et al (1982) Study on the structure, function and succession of the four types in natural secondary
299 forest. J Northeast For Univ 10:1–20
- 300 Chuvieco CE, Aguado I, Cocero D, et al (1999) Remote Sensing of Large Wildfires
- 301 Chuvieco E, Riaño D, Aguado I, Cocero D (2002) Estimation of fuel moisture content from multitemporal analysis of Landsat
302 Thematic Mapper reflectance data: Applications in fire danger assessment. Int J Remote Sens 23:2145–2162.
303 <https://doi.org/10.1080/01431160110069818>
- 304 De Groot WJ, Groot WJ De (1987) Interpreting the Canadian Forest Fire Weather Index (FWI) System. Fourth Cent Reg Fire
305 Weather Comm Sci Tech Semin Proceeding:3–14. <https://doi.org/citeulike-article-id:14176512>
- 306 De Jong MC, Wooster MJ, Kitchen K, et al (2016) Calibration and evaluation of the Canadian Forest Fire Weather Index (FWI)
307 System for improved wildland fire danger rating in the United Kingdom. Nat Hazards Earth Syst Sci 16:1217–1237.
308 <https://doi.org/10.5194/nhess-16-1217-2016>
- 309 De Melo-Abreu JP, Daldoum MA, Andrews PL, et al (2010) Applications of meteorology to forestry and non-forest trees. Geneva
310 WMO Guid to Agric Meteorol Pract
- 311 Di Giuseppe F, Pappenberger F, Wetterhall F, et al (2016) The potential predictability of fire danger provided by numerical
312 weather prediction. J Appl Meteorol Climatol 55:2469–2491. <https://doi.org/10.1175/JAMC-D-15-0297.1>
- 313 Dimitrakopoulos AP, Bemmerzouk AM, Mitsopoulos ID (2011) Evaluation of the Canadian fire weather index system in an
314 eastern Mediterranean environment. Meteorol Appl 18:83–93. <https://doi.org/10.1002/met.214>

315 Dimitrakopoulos AP, Papaioannou KK (2001) Flammability assessment of Mediterranean forest fuels. *Fire Technol* 37:143–152.
316 <https://doi.org/10.1023/A:1011641601076>

317 Dowdy AJ, Mills GA, Finkele K, de Groot W (2010) Index sensitivity analysis applied to the Canadian Forest Fire Weather Index
318 and the McArthur Forest Fire Danger Index. *Meteorol Appl* 17:298–312. <https://doi.org/10.1002/met.170>

319 Estes BL, Knapp EE, Skinner CN, Uzoh FCC (2012) Seasonal variation in surface fuel moisture between unthinned and thinned
320 mixed conifer forest, northern California, USA. *Int J Wildl Fire* 21:428–435. <https://doi.org/10.1071/WF11056>

321 Fernandes PM (2019) Variation in the canadian fire weather index thresholds for increasingly larger fires in Portugal. *Forests* 10:.
322 <https://doi.org/10.3390/f10100838>

323 Field RD (2020) Evaluation of Global Fire Weather Database reanalysis and short-term forecast products. *Nat Hazards Earth*
324 *Syst Sci* 20:1123–1147. <https://doi.org/10.5194/nhess-20-1123-2020>

325 Field RD, Spessa AC, Aziz NA, et al (2015) Development of a Global Fire Weather Database. *Nat Hazards Earth Syst Sci*
326 15:1407–1423. <https://doi.org/10.5194/nhess-15-1407-2015>

327 Flannigan MD, Krawchuk MA, De Groot WJ, et al (2009) Implications of changing climate for global wildland fire. *Int J Wildl*
328 *Fire* 18:483–507. <https://doi.org/10.1071/WF08187>

329 Flannigan MD, Logan KA, Amiro BD, et al (2005) Future area burned in Canada. *Clim Change* 72:1–16.
330 <https://doi.org/10.1007/s10584-005-5935-y>

331 Fujioka FM, Gill AM, Viegas DX, Wotton BM (2008) Chapter 21 Fire Danger and Fire Behavior Modeling Systems in Australia,
332 Europe, and North America. *Dev Environ Sci* 8:471–497. [https://doi.org/10.1016/S1474-8177\(08\)00021-1](https://doi.org/10.1016/S1474-8177(08)00021-1)

333 Good P, Moriondo M, Giannakopoulos C, Bindi M (2008) The meteorological conditions associated with extreme fire risk in
334 Italy and Greece: Relevance to climate model studies. *Int J Wildl Fire* 17:155–165. <https://doi.org/10.1071/WF07001>

335 Keane RE (2015) *Wildland fuel fundamentals and applications*. Springer

336 Lahaye S, Curt T, Fréjaville T, et al (2018) What are the drivers of dangerous fires in Mediterranean France? *Int J Wildl Fire*
337 27:155–163. <https://doi.org/10.1071/WF17087>

338 Li J, Song Y, Huang X, Li M (2015) Comparison of forest burned areas in mainland China derived from MCD45A1 and data
339 recorded in yearbooks from 2001 to 2011. *Int J Wildl Fire* 24:103–113. <https://doi.org/10.1071/WF14031>

340 Lynham TJ, Stocks BJ (1989) Suitability of the Canadian Forest Fire Damger Rating System for use in the Daxinganling Forestry
341 Management Bureau Heilongjiang Province, China. In: *Proceedings of the 10th Conference on Fire and Forest Whitewood=*
342 *Compte rendu du 10ieme Congress sur les incendies et la meterologie forestiere/editeurs DC Maiver, H. Auld, R.*
343 *Whitewood. Ottawa, Ont.? Forestry Canada 1989.*

344 Masinda MM, Li F, Liu Q, et al (2021) Prediction model of moisture content of dead fine fuel in forest plantations on Maoer
345 Mountain, Northeast China. *J For Res* 1–13

346 Masinda MM, Sun L, Wang G, Hu T (2020) Moisture content thresholds for ignition and rate of fire spread for various dead fuels
347 in northeast forest ecosystems of China. *J For Res*. <https://doi.org/10.1007/s11676-020-01162-2>

348 Matthews S (2014) Dead fuel moisture research: 1991–2012. *Int J Wildl Fire* 23:78–92. <https://doi.org/10.1071/WF13005>

349 Matthews S (2010) Effect of drying temperature on fuel moisture content measurements. *Int J Wildl Fire* 19:800–802.
350 <https://doi.org/10.1071/WF08188>

351 Nöchel J, Svennin JC (2017) Recent tree cover increases in eastern China linked to low, declining human pressure, steep
352 topography, and climatic conditions favoring tree growth. *PLoS One* 12:.
353 <https://doi.org/10.1371/journal.pone.0177552>

354 Papagiannaki K, Giannaros TM, Lykoudis S, et al (2020) Weather-related thresholds for wildfire danger in a Mediterranean
region: The case of Greece. *Agric For Meteorol* 291:108076. <https://doi.org/10.1016/j.agrformet.2020.108076>

355 Papakosta P, Straub D (2017) Probabilistic prediction of daily fire occurrence in the Mediterranean with readily available spatio-
356 temporal data. *IForest* 10:32–40. <https://doi.org/10.3832/ifor1686-009>

357 Rothermel RC (1972) A mathematical model for predicting fire spread in wildland fuels. Intermountain Forest & Range
358 Experiment Station, Forest Service, U.S. Dept. of Agriculture

359 Schunk C, Wastl C, Leuchner M, Menzel A (2017) Fine fuel moisture for site- and species-specific fire danger assessment in
360 comparison to fire danger indices. *Agric For Meteorol* 234–235:31–47. <https://doi.org/10.1016/j.agrformet.2016.12.007>

361 Simpson CC, Grant Pearce H, Sturman AP, Zawar-Reza P (2014) Behaviour of fire weather indices in the 2009-10 New Zealand
362 wildland fire season. *Int J Wildl Fire* 23:1147–1164. <https://doi.org/10.1071/WF12169>

363 Stocks BJ, Lynham TJ, Lawson BD, et al (1989) Canadian forest fire danger rating system: an overview. *For Chron* 65:258–265

364 Thomas B (1990) The Jiagedaqi Project: forest fire control in China. *For Chron* 66:266–270. <https://doi.org/10.5558/tfc66266-3>

365 Tian X, McRae DJ, Jin J, et al (2011) Wildfires and the Canadian forest fire weather index system for the Daxing'anling region
366 of China. *Int J Wildl Fire* 20:963–973. <https://doi.org/10.1071/WF09120>

367 Tian XR, Zhao FJ, Shu LF, Wang MY (2014) Changes in forest fire danger for south-western China in the 21st century. *Int J*
368 *Wildl Fire* 23:185–195. <https://doi.org/10.1071/WF13014>

369 Tosic I, Mladjan D, Gavrilov MB, et al (2019) Potential influence of meteorological variables on forest fire risk in Serbia during
370 the period 2000-2017. *Open Geosci* 11:414–425. <https://doi.org/10.1515/geo-2019-0033>

371 Tremblay PO, Duchesne T, Cumming SG (2018) Survival analysis and classification methods for forest fire size. *PLoS One*
372 13:1–16. <https://doi.org/10.1371/journal.pone.0189860>

373 Tsinko Y, Bakhshaii A, Johnson EA, Martin YE (2018) Comparisons of fire weather indices using Canadian raw and
374 homogenized weather data. *Agric For Meteorol* 262:110–119. <https://doi.org/10.1016/j.agrformet.2018.07.005>

375 Van Wagner CE (1987) Development and structure of the Canadian forest fire weather index system

376 Van Wagner CE (1974) Structure of the Canadian Forest Weather Index. *Dep Environ Can For Serv*

377 Vitolo C, Di Giuseppe F, Krzeminski B, San-Miguel-ayanz J (2019) Data descriptor: A 1980–2018 global fire danger re-analysis
378 dataset for the Canadian fire weather indices. *Sci Data* 6:1–10. <https://doi.org/10.1038/sdata.2019.32>

379 Wang AX, Cantin A, Parisien M, et al (2019) Package ‘cffdrs’

380 Wang C (2006) Biomass allometric equations for 10 co-occurring tree species in Chinese temperate forests. *For Ecol Manage*
381 222:9–16. <https://doi.org/10.1016/j.foreco.2005.10.074>

382 Wotton BM (2009) Interpreting and using outputs from the Canadian Forest Fire Danger Rating System in research applications.
383 *Environ Ecol Stat* 16:107–131. <https://doi.org/10.1007/s10651-007-0084-2>

384 Wu Z, He HS, Keane RE, et al (2020) Current and future patterns of forest fire occurrence in China. *Int J Wildl Fire* 29:104–119.
385 <https://doi.org/10.1071/WF19039>

386 Xanthopoulos G, Roussos A, Giannakopoulos C, et al (2014) Investigation of the weather conditions leading to large forest fires
387 in the area around Athens, Greece. *Parte*: <http://hdl.handle.net/103162/34013>

388 Yang G, Di X (2011) Adaptation of Canadian Forest Fire Weather Index system and its application. *Proc - 2011 IEEE Int Conf*
389 *Comput Sci Autom Eng CSAE 2011* 2:55–58. <https://doi.org/10.1109/CSAE.2011.5952422>

390 Yang G, Di XY, Zeng T, et al (2010) Prediction of area burned under climatic change scenarios: A case study in the Great Xing'an
391 Mountains boreal forest. *J For Res* 21:213–218. <https://doi.org/10.1007/s11676-010-0035-x>

392 Ying L, Han J, Du Y, Shen Z (2018) Forest fire characteristics in China: Spatial patterns and determinants with thresholds. *For*
393 *Ecol Manage* 424:345–354. <https://doi.org/10.1016/j.foreco.2018.05.020>

394 Zhang J, Cui X, Wei R, et al (2017) Evaluating the applicability of predicting dead fine fuel moisture based on the hourly Fine

395 Fuel Moisture Code in the south-eastern Great Xing'an Mountains of China. *Int J Wildl Fire* 26:167–175.
396 <https://doi.org/10.1071/WF16040>

397 Zhang JH, Yao FM, Liu C, et al (2011) Detection, emission estimation and risk prediction of forest fires in China using satellite
398 sensors and simulation models in the past three decades-An overview. *Int J Environ Res Public Health* 8:3156–3178.
399 <https://doi.org/10.3390/ijerph8083156>

400 Zong X, Tian X, Wang X (2021) An optimal firebreak design for the boreal forest of China. *Sci Total Environ* 781:146822.
401 <https://doi.org/10.1016/j.scitotenv.2021.146822>

402 Zylstra PJ (2011) Forest flammability: modelling and managing a complex system. 435. <https://doi.org/10.13140/2.1.3722.0166>
403

Figures

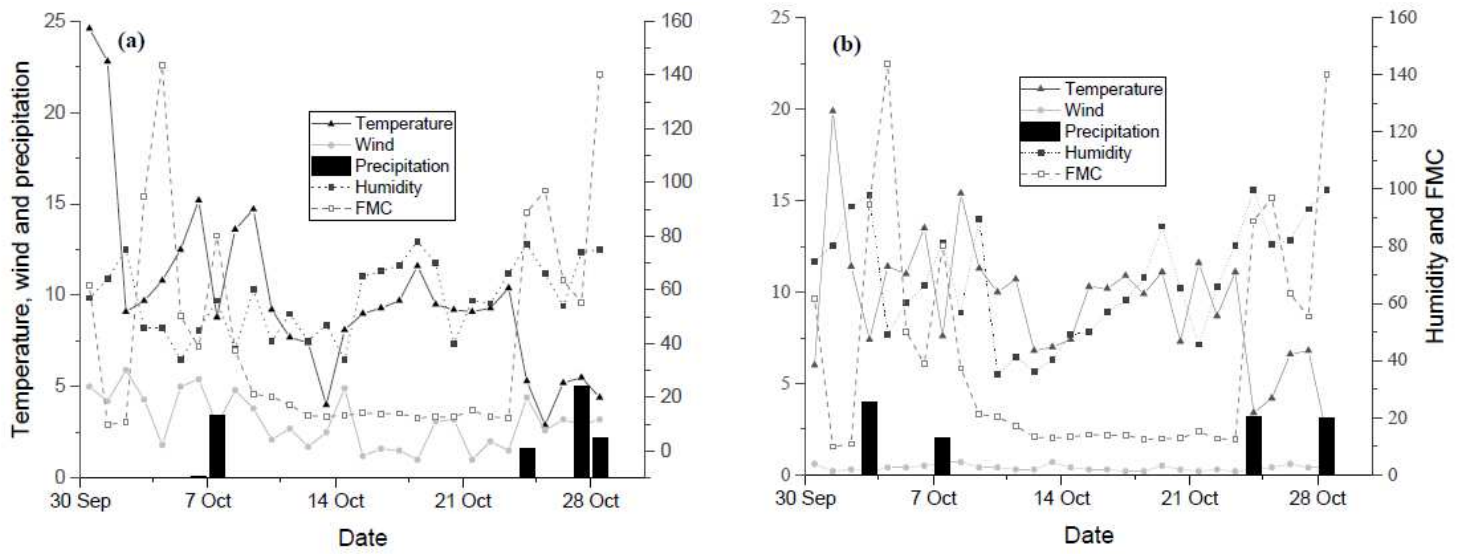


Figure 1

Variation of FMC based on (a) FMC meter and (b) China Weather Station database

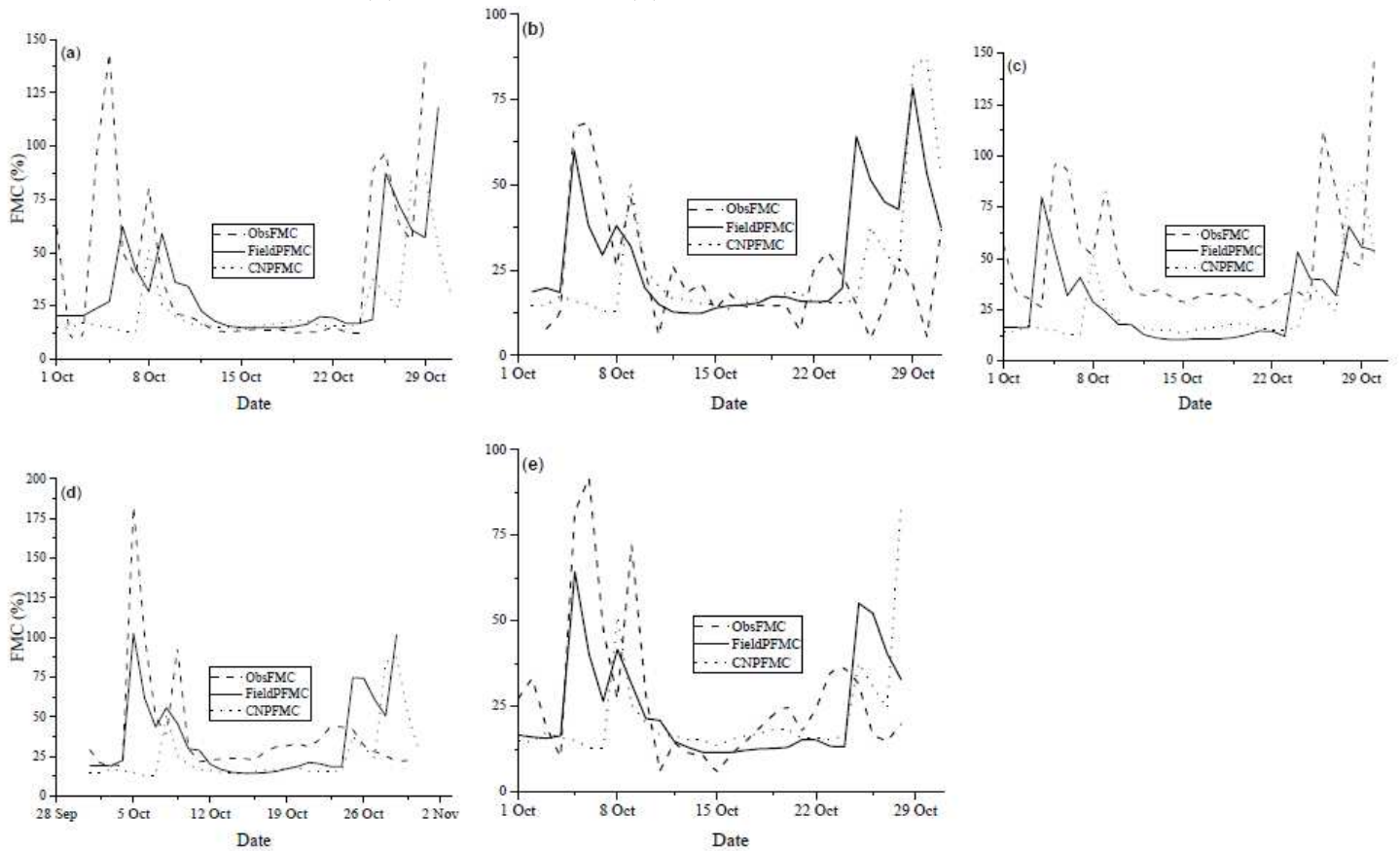


Figure 2

a, b, c, d, e Observed versus FMC meter and CWS predicted FMC, in 2019

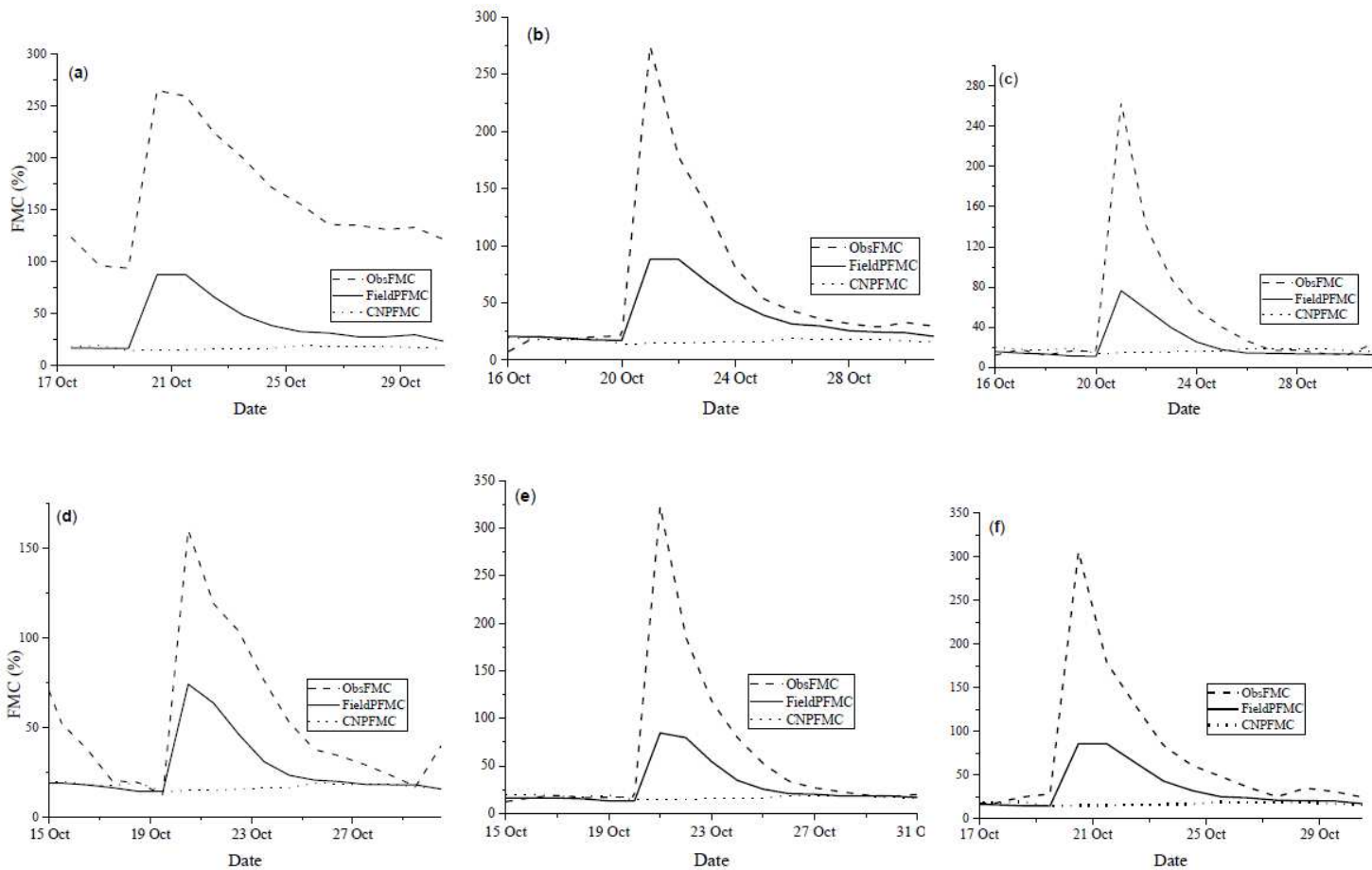


Figure 3

a, b, c, d, e, f Observed versus FMC meter and CWSS predicted FMC, in 2020

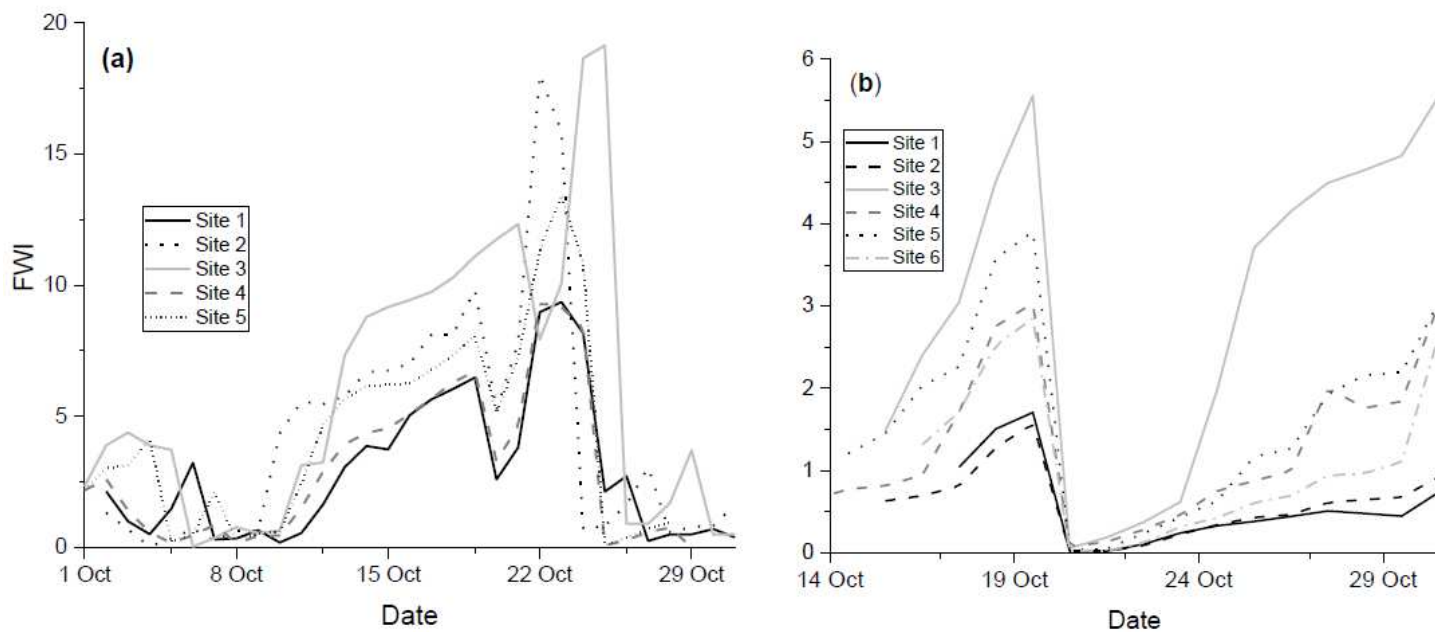


Figure 4

Variation of FWI in 2019 (a) and 2020 (b)